

AD-A055 316

NAVAL SHIP ENGINEERING CENTER WASHINGTON DC
CERAMIC GAS TURBINE ENGINE DEVELOPMENT.(U)
1977 J W FAIRBANKS

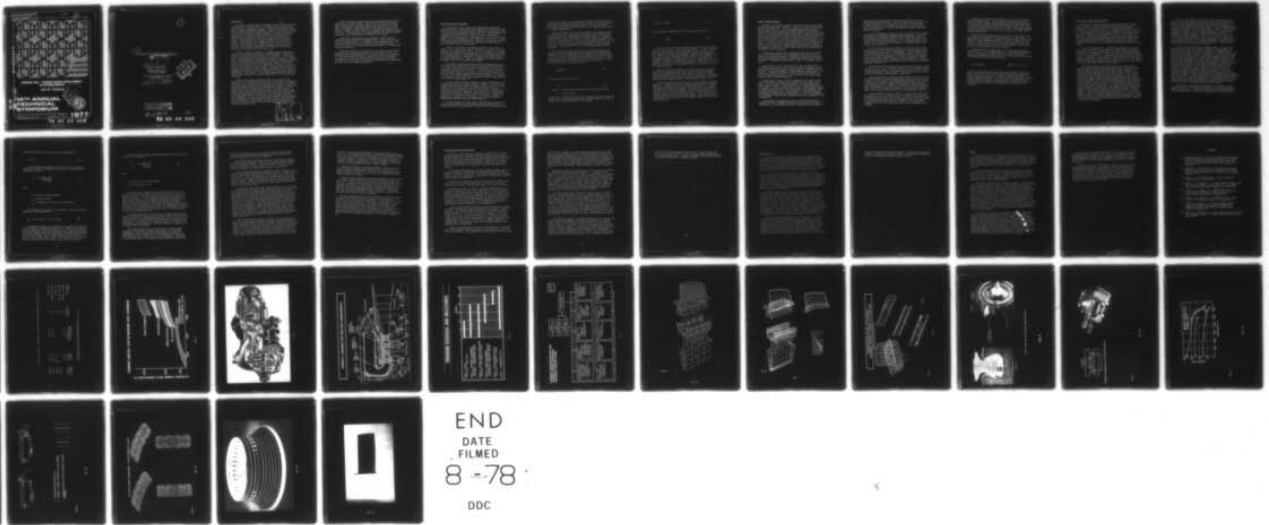
F/G 13/10

UNCLASSIFIED

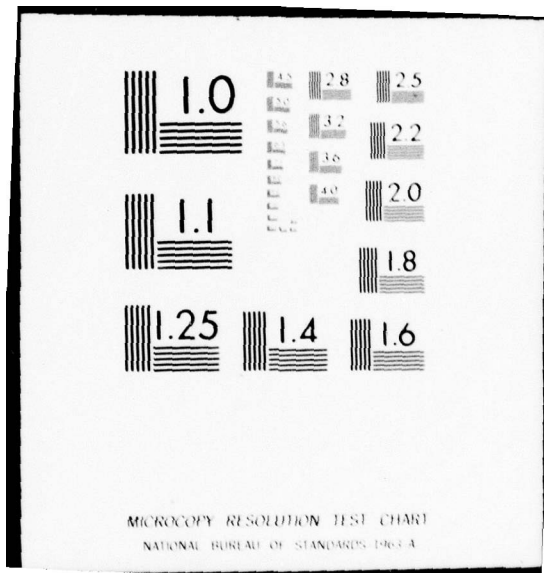
NL

1 of 1

AD
A055 316



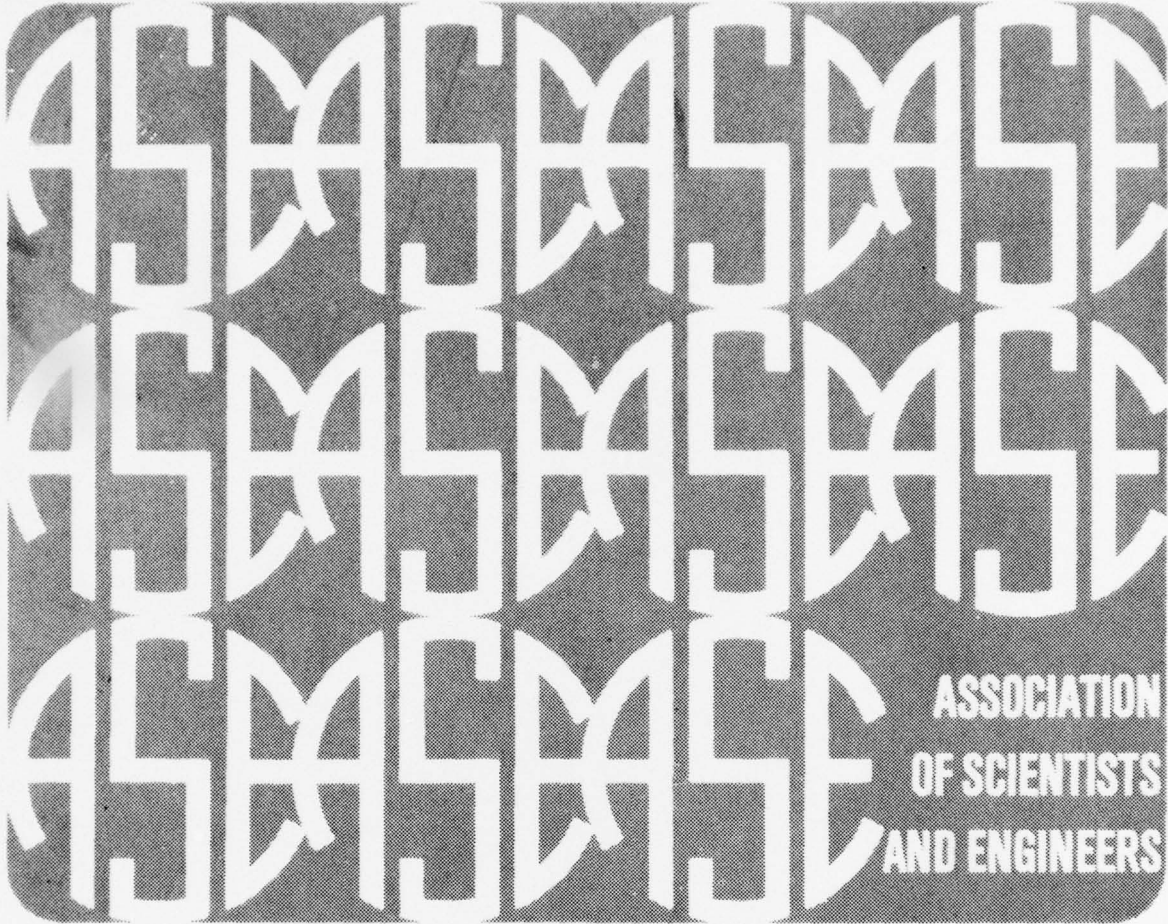
END
DATE
FILMED
8 -78
DDC



This document has been approved for public release and sale; its distribution is unlimited.

✓ (D) 2

AD A 055316



**CERAMIC GAS - TURBINE ENGINE DEVELOPMENT,
AN INTERIM REPORT**

John W. Fairbanks



AU NO
DDC FILE COPY

**14TH ANNUAL
TECHNICAL
SYMPOSIUM**

ASSOCIATION OF SCIENTISTS AND ENGINEERS OF
THE NAVAL AIR AND SEA SYSTEMS COMMAND
DEPARTMENT OF THE NAVY - WASHINGTON, D.C. 20360

1977

78 06 09 048

①

⑥

CERAMIC GAS TURBINE ENGINE DEVELOPMENT.
AN INTERIM REPORT.

⑨

By

⑩

JOHN W. FAIRBANKS

INTERNAL COMBUSTION AND
GAS TURBINE BRANCH

NAVAL SHIP ENGINEERING CENTER
WASHINGTON, DC

DDC
JUN 19 1978
NAVY

⑪ 1977

⑫ 46p.

This document has been approved
for public release and sale; its
distribution is unlimited.

401 499

LB

78 06 09 048

INTRODUCTION

Why develop a ceramic marine gas turbine engine? Justification for the allocation of major resources to develop the ceramic gas turbine engine requires a reasonable prospect of obtaining significant improvements in engine performance, durability, reduction in critical materials use, and cost savings on a comparative basis to current-art metal gas turbine engines. Improved engine durability at existing operating conditions is the Navy's top priority for materials development. Ceramics have much greater resistance to hot-corrosion than metal alloys. Hot-corrosion of hot-section components is life-limiting engines. Ceramic hot-section components would be much more able to withstand hot-streaking, i.e., carbon burning on the vane air foil surface. These corrosion and thermal properties of ceramics would provide a much expanded tolerance for fuel impurities or with the synthetic fuels anticipated in the 1980's.

The Navy is vitally interested in improving engine performance to extend ships operational availability and fuel economy. Engine efficiency is related to the gas turbine inlet temperature. The capabilities of metal superalloys and ceramics are shown in Figure 1. Development of superalloys for turbine airfoils appears to be approaching their limits with directionally solidified (DS) and single crystal airfoils. Airfoils for the Navy's high power marine gas turbines such as the LM 2500 (20,000 HP) and the FT9 (33,000-50,000 HP range) use thin-wall airfoils with intricate cooling schemes. Internally these airfoils use impingement and convective heat transfer and externally film cooling is obtained with bleed air introduced through a series of holes along the leading edge of the airfoil. These blade cooling techniques reduce the airfoil metal temperature as much as 600°F below that of the gas path temperature.

However, these advanced cooling schemes use air bled off the compressor, which reduces engine efficiency and introduces manufacturing complexities for channeling the cooling air to the airfoils. Leading edge cooling holes can encounter hole plugging in marine use which leads to reduced engine performance and possible airfoil failure. Smaller engines in the 1,000 HP range generally don't use blade cooling. In either event, solid ceramic blades and vanes that could operate without cooling with gas path temperatures of 2200°F could provide tremendous performance improvements. Specifically, the FT9 engine would have a power improvement of 30% and a specific fuel consumption (SFC) reduction of 7% compared to the metal engine with same turbine inlet temperature. Garrett indicates the T76 with solid ceramic airfoils replacing the current solid metal airfoils would improve engine output power by 40% and reduce the SFC by 10%.

ACCESSION for	White Section <input checked="" type="checkbox"/>	Buff Section <input type="checkbox"/>	<input type="checkbox"/>
NTIS	DDC	UNANNOUNCED	JCS FILED
		<i>Per</i>	<i>Director</i>
BY	DISTRIBUTION/AVAILABILITY CODES		Dist.
			<i>A</i>

Today's metal gas turbine engines require considerable amounts of metals such as chromium, cobalt, columbium and nickel which are relatively expensive and in limited supply. Also, the sources for these metals are in areas of potential political instability. On the other hand, the candidate ceramic materials for the engine application are silicon, nitrogen and carbon which are inexpensive raw materials abundant in the U.S. The realizable cost savings potential for ceramic turbine components requires achievement of advances in processing.

Ceramic gas turbines should be considerably lighter and more compact than metal engines of comparable power. These features are of particular significance for the advanced, non-displacement hull, high-performance ships, helicopters, remotely piloted vehicles (RPV), missiles as well as for conventional surface combatants' propulsion and electrical generators.

While these payoffs for successful use of ceramics in gas turbine engines must be classified very high on any desirability scale, the problems confronting implementation of the structural use of ceramics for these applications also have a commensurate level of difficulty. It is worthwhile to look into the structure and properties of ceramic materials in order to appreciate the special design techniques necessary for their use in the engine application.

DESIGN WITH BRITTLE MATERIALS

The structural use of ceramic materials involves design with brittle materials. Unfortunately, many engineers and most laymen make the mistake of considering brittleness synonymous with fragility. There is a very important distinction between the two. Brittleness describes a material that fractures with little or no plastic deformation. Fragility is a property which is characterized by fracture at very low stress with little deformation. Some materials, such as those children knock off gift shop display counters, combine both properties. However, the ceramic materials of interest for engineering applications are brittle materials that are not fragile.

Fragility is avoided if a material can absorb a large amount of energy. Thus, ceramic armor used by aircrews in Viet Nam is a brittle material, but certainly not fragile. In fact this same type of ceramic armor (boron carbide) is used extensively in the President's helicopter. This distinction can be further appreciated by considering rubber which is a brittle material but certainly not fragile as it shows a large extension before failure. Godfrey has proposed the word "inductility" to replace "brittle" to describe this property.

The problems that brittle materials pose for engineering use is that local stress concentrations are not relieved by plastic yielding as is the case with metals and the strength distribution of ceramics is considerably wider compared to metals. This variability in properties and the susceptibility to fracture due to stress concentrations introduces much more complex design problems with ceramics than with metals. In order to use ceramic materials as load bearing members in a design, it is necessary to precisely analyze component stresses using techniques such as finite element analysis.

Since the high temperature strength to weight characteristic and Young's Modulus per unit weight of certain ceramics is of interest for engineering application, consider bonding strength of atoms. A perfect crystal is one with regularly spaced pattern of atoms in planes. Resistance to cleavage fracture, or the pulling apart of the atoms in a direction normal to the atom planes, and to shear, the sliding across atom planes in parallel, depends on the atomic forces. Although the strength of most materials are limited by the presence of faults, the principles of interest can be illustrated by the ideal strengths of flawless materials from an atomic bond perspective.

In metal crystals, the atoms tend to lose electrons from the outer shells and the positive ions thus formed are held together by free electrons produced by the separation. As the face of a cleavage fracture

plane are pulled apart, the bonds between the atoms in the two planes are stretched against the tensile forces in them. The work done in this stretching of the bonds accumulates energy. The total work done on these bonds becomes the surface energy of the two cleaved forces, which is a measurable parameter.

However in metals, when forces are applied in the shearing mode, the atoms slide over one another along the shear plane and their bonds are made and broken in succession with neighbor atoms in the opposite parallel plane. Since these bonds at the shear planes are repeatedly renewed, the shear strength is lower than the cleavage strength. On the other hand, materials such as sapphire, diamond and titanium carbide, in which the atoms are held together by covalent bonds, have high shear resistance. Covalent bonds are formed by neighboring atoms sharing electrons.

The concept of strength and flaw size is of major concern with ceramics as it plays an important role in design and non-destructive examination (NDE). Consider a block of ceramic in pure tension which has a crack with an approximately circular region of radius "r" in the center of the crack. The presence of the crack releases the region of the crack from stress and hence relieves it of strain energy. If the applied stress is σ , this elastic energy is:

$$\frac{\pi r^2 \sigma^2}{E} \quad (1)$$

The surface energy at the crack is:

$$4\gamma r \quad (2)$$

where γ = surface energy per unit area in the fracture plane

E = Young's modulus

The factor 4 is used because there are two growing surfaces at each end of the crack. The crack can grow if the elastic energy is at least as large as the rate of increase of surface energy:

$$\frac{d}{dr} \left(4\gamma r - \frac{\pi r^2 \sigma^2}{E} \right) = 0 \quad (3)$$

Thus, the fracture strength, which is the applied stress, is:

$$\sigma = \sqrt{\frac{E\gamma}{r}} \quad (4)$$

This is the famous Griffith formula that shows that, in the ideal case of no flaws, which is the special case where $r = a$, the interatomic spacing, the theoretical fracture strength of Si_3N_4 is about 4×10^6 psi. However, in practice Si_3N_4 materials have fracture strength of about 1/100 of the theoretical strength. Actually, with materials such as hot-pressed Si_3N_4 , the largest internal flaw at a stress level determines the time of brittle failure. Thus, if the design life of a component is defined at a temperature, then the largest flaw size or the allowable stress level terms are interchangeable. That is to say, a 0.030 inch internal flaw or an allowable stress of 16,000 psi at 2200°F are equivalent terms.

Materials with high strength in all directions are of particular interest for engineering application. Basic considerations suggest polycrystalline materials with a high density of strongly covalent bonded atoms approaching random grain orientation would be of interest. The high strength to weight and stiffness to weight ratios of covalent bonded materials suggests them over those formed with ionic bonds.

Strength characteristics derived from covalent bonded atoms would appear to be related to the size of the atom and the number of valence electrons. Following this logic, the small atoms with 3 or 4 valence electrons which form covalent bonds in several directions around each atom would be of particular interest. The atoms in the part of the Periodic Table that have these characteristics include beryllium, boron, carbon, nitrogen, oxygen, aluminum and silicon. The strongest solids generally contain one or more of these elements. This group contains the elements of the ceramic materials currently being developed for gas turbine engine use.

CERAMIC TURBINE MATERIALS

Basically, two chemical compounds provide the basis of the present ceramic turbine materials technology. These are silicon nitride (Si_3N_4) and silicon carbide (SiC). The SiC materials have higher intrinsic refractoriness, Young's modulus and thermal expansion coefficients. However, the lower thermal expansion coefficient of Si_3N_4 , provides good resistance to thermal stresses and thermal shocks encountered in the gas turbine engine application. Thermal expansivity controls the thermal expansion strain which is produced by a given temperature gradient. The elastic properties of the material determine the stress produced by this strain. Thus, the transient stresses developed in a gas turbine during start up, shut down, load variations and hot-streaking are strongly dependent on the material's thermal expansivity and elastic properties. The mechanical properties of both SiC and Si_3N_4 are very significantly determined by their processing.

There are two commonly used processing methods for SiC and Si_3N_4 . These are hot-pressing and reaction sintering. The latter is also referred to as reaction bonded. In addition, there are two less developed processing methods, additive sintering and chemical vapor deposition (CVD). Representative properties of Si_3N_4 are included as Tables I and II.

Hot-pressing is usually done with dies that are restricted to rudimentary block shapes. Blade airfoil and root attachments contours must be machined most commonly by diamond abrasive procedures which are expensive. Hot-pressing produces ceramic materials that approach zero porosity or theoretical density. Hot-pressed Si_3N_4 (HPSN) which is close to theoretical density, 3.2 g/cc, is a very hard, high strength material with low thermal expansivity.

Hot-pressing of Si_3N_4 is done in essentially five steps. Since Si_3N_4 does not occur in nature, the process must start with silicon metal. Lump silicon is crushed and milled to a loose powder which is then nitrided at 1350°C. The resulting Si_3N_4 is crushed and milled to a fine powder. A densifying agent, such as a few percent magnesia (MgO), is milled together with this fine Si_3N_4 powder. This resulting powder is pressed in graphite dies to about 1750°C to a block form roughly encompassing the desired final configuration. It is the high hardness of the HPSN part which requires extensive machining to the desired final configuration.

Unfortunately, the magnesia additive in HPSN also contributes to a significant loss of strength, fatigue and creep resistance at high temperatures. These mechanical property limitations are attributed to a

second phase involving the additive, which is probably a silicate, formed at the grain boundaries. This silicate phase becomes more fluid at higher temperatures. Improvement in the HPSN is being pursued through variations in the thickness and composition of this silicate phase in the boundaries in order to increase the silicate viscosity at higher temperatures.

Two recent approaches to improve the refractoriness of the silicate bonding phase at elevated temperatures appear promising. Work at the Army Materials and Mechanics Research Center (AMMRC) has shown that substituting a yttrium oxide (Y_2O_3) in place of the MgO produces much improved strength at high temperature (3). Preliminary results at NRL suggest that a zirconia densifying additive is also beneficial for hot strength improvement (8).

Reaction bonding involves a reaction of free silicon with either nitrogen or carbon even though applications vary between Si_3N_4 and SiC and even within various types of these bodies. In the reaction bonded Si_3N_4 (RBSN) process the body of silicon metal powder is formed precisely to the desired shape which is referred to as the green casting. The green casting is then heated in a nitrogen atmosphere at temperatures between $1250^{\circ}C$ - $1450^{\circ}C$. Generally iron is included as a catalyst. Resulting RBSN bodies characteristically retain their green casting part dimensions within 0.10%.

Several methods of compacting silicon powder to form green castings are used, such as: die or isostatic pressing, injection molding, flame-spraying and slip casting. Molding appears to be particularly suitable for mass production of complex shapes. Flame-spraying and slip-casting produce lower porosity than molding or pressing (2).

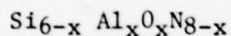
Characteristically the RBSN parts have between 20% to 30% porosity, which limits their low temperature strengths to less than half of that of HPSN. This is because in the RBSN process diffusion of the reacting nitrogen gas is reduced as densification proceeds, which results in isolated unreacted sites. However, the absence of densifying additives allows maintenance of strength and creep resistance at high temperatures without the temperature limiting drop off encountered with HPSN. RBSN is less expensive than HPSN as much less machining is required.

Reaction bonded SiC (RBSC) is made in a similar manner as the RBSN. Molten silicon (Si) is reacted with a body of carbon (C), often with substantial SiC particles, to form RBSC. Porosities of the RBSC bodies are much lower than in the RBSN but strengths are about the same due to the combination of porosity and free Si and/or C left in the body. Presence of free Si in the body also limits the high temperature performance.

Additive sintering involves some aspects of the hot-pressing and reaction bonded processes. In the additive sintering process Si_3N_4 powders with MgO or other densifying additives similar to those used in hot-pressing are sintered. The resultant properties are between those of hot-pressed and reaction bonded bodies, though closer to the former. Porosities have been obtained as low as 1% to 5%. The primary advantage of additive sintering is its lower cost, especially for larger and/or complex shaped parts.

Chemical vapor depositing (CVD) can be used to coat ceramic structural parts or form monolithic bulk parts often in complex shapes. CVD coating provides a method of obtaining zero porosity without the use of additives. These coatings applied over a machined ceramic body would assist in reducing the effects of the surface flaws which result from grinding. The end result would be increased strength. CVD is one of the more promising processes being investigated.

Considerable work is being done on a class of materials called Sialons in the U.S., UK, Germany and Japan. It has been suggested that some of these materials are equivalent to or better than Si_3N_4 in mechanical strength and chemical stability. The name Sialon was derived as an abbreviation for the chemical formula:



(where $x = 0$ to 4.8.)

The Sialon material has a variable molecular composition in which over half of the silicon nitride can be replaced with aluminum oxynitride, without altering the structure and without changing properties of the silicon nitride drastically (1). Sialon's can be hot-pressed or sintered to near theoretical density. Thus, the Sialon's hold the promise of similar hardness and strength characteristics of the HPSN, but they can be formed much more closely to the desired final configuration by sintering.

DARPA/NAVSEA CERAMIC ENGINE PROGRAM

Development of ceramic materials, principally Si_3N_4 , to the point where it could be considered as an engineering structural material emanated from work done by Norm Parr at the Admiralty Materials Laboratory in the UK in the fifties. In the late 1960's Parr projected use of ceramic components in gas turbine engines and identified many of the design precepts that were necessary in order to design with brittle materials. However, the program that deserves the major credit for developing ceramic design technology for gas turbine structural applications is the Defense Advanced Research Projects Agency (DARPA) sponsored program begun in 1971 with Ford and Westinghouse, which was technically monitored by the Army Material and Mechanics Research Center (AMMRC).

The goal of the DARPA/Ford - Westinghouse program was to prove by a practical demonstration that efforts in ceramic design, materials, fabrication, testing and evaluation can be drawn together and developed to establish the usefulness of brittle materials for engineering applications. This application of ceramics was directed at two very different types of gas turbines. Ford developed a small vehicular turbine with a nominal 200 HP rating using an entire ceramic hot flow path. Westinghouse worked on ceramic first stage vanes and design studies of ceramic rotors for a large stationary turbine of about 30MW (4).

Considerable progress was made in ceramic materials characterization, brittle material design techniques, ceramic component testing and non-destructive examination (NDE) during these programs. The ceramic technology developed on this DARPA project coupled with some excellent work accomplished with the support of NASA - Lewis and the British Ministry of Defense provided a technology base to launch a second DARPA ceramic gas turbine engine development program. DARPA's second major engine program involved developing ceramic structural hot-section components for the Garrett T76 engine which is shown in Figure 2. Successful application of ceramics in this engine would analytically improve engine power output from 715 to about 1000 HP with a 10% reduction in specific fuel consumption. The components being designed with ceramics are the first and second stage blades and vanes, the annular combustor, the transition pieces and the turbine shrouds as shown in Figure 3. DARPA has obtained Garrett agreement for a 3 year program funded at \$12.5M. The program schedule is outlined in Figure 4. DARPA tasked the Naval Sea Systems Command (NAVSEA) to manage the program who in turn directed the Naval Ship Engineering Center (NAVSEC) to technically monitor the program.

Success of the program is defined by DARPA as accomplishing 50 hours of test stand operation and 10 hours operation with the ceramic engine on specified power profile propelling an appropriate boat. This success criteria suggests that ceramic state-of-the-art technology is not ready to challenge metal engines, except in short life engines where weight and efficiency are major considerations. However, the potential advantages of ceramic over metal engine components is tremendous and justifies reasonable efforts in developing ceramic technology. This DARPA/Garrett program should be viewed as an evolutionary step in a revolutionary design technology. Thus, a major output of this program is the design logic track used and the assessment of the relevance of the techniques employed. A new technical management concept was developed by NAVSEC for this program, which is referred to as the Technical Review Panel for the Ceramic Engine Program.

This Technical Review Panel is somewhat similar to a NASA Flight Readiness Review Team. The members are experts from Government activities actively involved in ceramic technology or advanced stress analysis as indicated in Figure 5. The intent of the Panel is to insure that Government supported ceramic technology is accurately evaluated for use in the Garrett program. The panel attends program milestone review meetings and additional sessions with Garrett engineers working in the area of their specialization. Ceramic materials specialists on the Panel are also conducting characterization testing of candidate materials procured through Garrett. This testing will augment the sparse data base, which is necessary for meaningful statistical analysis, and validate the Garrett test data. Comments from the review panel are collated by NAVSEC and discussed with the contractor. Thus, this technical management concept has drastically reduced the tendency to "reinvent-the-wheel". Time and money constraints require use of ceramic materials available in quantity and adaption of promising design approaches from earlier work. Garrett's challenge is to effectively integrate the state-of-the-art ceramic technology into a hot-section design. Analytical techniques, design, NDE, proof-testing, component testing and engine testing should all be extended beyond what has been done.

The Technical Review Panel participation is also aimed at developing DOD in-house capability for assessing use of ceramic technology in advanced applications. Tracking the design logic and testing should enhance capabilities of directing R&D program directions and definition.

ENGINE MATERIAL SELECTION

The time constraint of the DARPA/NAVSEA Ceramic Gas Turbine Engine program schedule and the defined objective of successfully operating the ceramic engine for 60 hours strongly influenced material selection. A HPSN with the MgO additive, specifically Norton NC-132, was chosen as the primary candidate ceramic material for the first and second stage blades. The NC-132 material is one of the most extensively tested ceramic materials. The manufacturer has considerable experience making NC-132 which should reduce quality control problems and minimize late delivery risks. Available data indicates NC-132 can perform the program objectives with a high probability of success. The high temperature strength and creep resistance characteristic of the MgO densified NC-132 has limited the average turbine inlet temperature to 2200°F. The estimated time where creep rupture becomes a concern with first stage blades of NC-132 is on the order of 210 hours and for the second stage blades is 600 hours. However, loss of the necessary blade tip-shroud clearances due to creep, coupled with corrosion/oxidation effects building up in long term use, also is a potential life limiting problem.

A HPSN containing 8% yttrium oxide (Y_2O_3) is back-up blade material which will be brought through material characterization testing. This material is reported to have higher strength at high temperature and greater creep rupture resistance than NC-132. Sufficient data are not available to fully assess the yttria densified material for the Garrett engine.

The other ceramic components, the first and second stage vanes, the annular combustion chamber, transition pieces and shroud are all being designed with RBSN as the primary candidate. These parts are large and/or more complex than the blades but will encounter lower stresses.

CERAMIC TURBINE BLADE DESIGN

Very precise thermal and stress-analysis techniques are required to identify local stress concentrations in ceramic turbine blades and vanes. Design iterations are necessary to reduce these stress levels to within the capability of the material including a design margin. Numerical methods, principally 2-D and 3-D finite element analysis techniques, are employed. In addition to the conventional design criteria, the structural use of ceramics as highly stressed components requires a statistical analysis for the failure probability, or in a more positive sense, the probability of success.

Fracture in some ceramics, particularly in the fully dense materials, is directly related to slow crack growth, as previously discussed. From a designer's perspective, the flaw size and distribution are important insofar as they account for a large variability in strength of ceramics. It should also be intuitive that enlarging the component size would increase the probability of containing a large flaw. Stress distribution is very important. If a component is under uniform tensile stress then it has a higher probability of failing at its largest flaw than it would have with only a small section under a much higher stress. The Weibull strength distribution is the most commonly used approach for ceramic material lifetime predictions in structural application.

The Weibull distribution function is expressed as equation (5):

$$P_F = 1 - e - \left[\frac{(\sigma_o - \sigma_u)}{(\sigma_o - \sigma_u)} \right]^M, \quad (5)$$

where:

P_F = Probability of failure

σ_u = Lower bound strength (lowest possible strength)

σ_o = Characteristic strength

M = Weibull slope

Since the probability of success (P_s) can be expressed as:

$$P_s = 1 - P_f \quad (6)$$

Garrett modified the Weibull distribution for use with finite analysis such that the probability of success of a given element is expressed as follows:

$$P_{s_e} = e^{-v/v_t} \left[\frac{(\sigma - \sigma_u)}{(\sigma_o - \sigma_u)} \right]^M \quad (7)$$

where:

v = volume of a finite element

v_t = stressed volume

P_{s_e} = probability of success of finite element

The probability of success of the component is found by combining individual local probabilities:

$$P_{s_T} = (P_s)_i (P_s)_{i+1} \dots (P_s)_M \quad (8)$$

The Weibull function, M , is a measure of the scatter or dispersion of the distribution somewhat analogous to the standard deviation of a normal distribution. The Weibull function, M , is obtained by plotting on log-log "Weibull paper" with logarithmic scales that yield straight lines and coordinates that show the percent of original parts that fail as a function of time. Small M values represent a large degree of scatter. Most ceramics have M values in the range of 4 to 15, whereas metals are estimated to have M values in the 50 to 100 range (5).

Garrett also used a Weibull distribution approach for surface area effects with the equation:

$$P_{s_e} = e^{-a/a_t \left[\frac{\sigma - \sigma_u}{\sigma_o - \sigma_u} \right]^M} \quad (9)$$

where:

a = surface area of a finite element

a_t = stressed surface area.

The probability of success in a local volume or surface, i.e., for a particular finite element, requires consideration of the three principal stresses. The total probability of success is assumed to be equal to the product of the individual probabilities associated with each principal stress. Since compressive strength of ceramics is an order of magnitude greater than tensile strength and compressive stresses contribute little to crack growth, compressive stress was not analyzed. Thus, the probability of success of a component was taken as the product of two Weibull distributions of the probabilities of success of all the local volumes and surface areas which are readily obtained with finite element analysis (5).

The Weibull distribution is based on the assumption that a single flaw in the elemental volume produces fracture. While the validity of this assumption can be challenged, experimental data is used to fit the equation. Thus, an extensive data base is required covering the range of interest. Unfortunately, this data base does not yet exist but is being developed in this program. Component testing is a mandatory step in ceramic engine development.

The ceramic turbine blade design began with a finite element approach to establish the optimum airfoil shape for the gas path aerodynamics. The first and second stage blades were designed to accommodate transient stresses for the cold engine start and steady state operation with a 2200°F turbine inlet temperature. Representative analytical models of 3D thermal and stress analysis on the blade

and attachment region to the metal disk are shown as Figures 6 and 7. A series of design iterations were necessary to reduce local stress levels to provide a 99.98 success probability.

Traditional design techniques were used to reduce stress concentrations in these iterations. Blade twist was reduced several degrees from the aerodynamic optimum. The airfoil trailing edge was thickened and the leading edge was made a little more blunt. Fillets at the platform were made with more gradual contours or longer radii.

Typical stress distributions resulting from these iterative techniques for the second stage blade is shown in Figure 8. Maximum stresses are in the blade near the platform in the mid-span area of the airfoil suction side. Stress concentrations in the leading edge and trailing edge were kept low enough with margin for thermal shock and vibration induced stresses. Blade bending frequency was kept significantly higher than the stator wake passage frequency at design speed, thereby minimizing vibratory excitation (5).

A conventional metal gas turbine blade attachment to the disk could not be used because the stress levels resulting from the ceramic blade and metal disk thermal expansion mismatch would be too high. The Westinghouse and Pratt and Whitney ceramic blade dovetail root attachment design using a compliant layer was investigated and adopted with modifications. The blade root attachment must accommodate the centrifugal force, thermal stresses and gas bending forces. Critical to the attachment is the blade - disk contact area which must distribute the stresses over a wide area. Even highly polished surfaces have microscopic protuberances which become localized points of contact upon mating two such surfaces. Metals distribute stresses fairly well so these surface protuberances are not a significant mechanical problem with a decent surface finish. However, high strength ceramics are limited in their ability to accommodate the local stress concentrations caused by the microscopic surface protuberances, because of their limited plasticity.

This contact problem appears to be solvable by the introduction of a metal foil at the interface between the ceramic and the mating metal part, which would initially plastically deform, increasing the physical contact area between the ceramic and the metal, thereby distributing the contact stresses. Platinum (Pt) appeared to be a promising compliant layer in the Pratt and Whitney work and was consequently tested by Garrett. A dovetail root attachment with Pt compliant layers in both contact areas is shown in Figure 9 along with the spin-pit test disk. Garrett cold and hot spin test results indicates that Pt might extrude

too much for long term engine operation, but would probably be satisfactory for the demonstration testing. Stainless steel compliant layers appear in early testing to be more resistant to extrusion while adequate for initial plastic deformation, even though they anneal with high temperature exposure. Additional testing is necessary to finalize and validate the blade attachment design. However, progress to date indicates the blade attachment will not be a "show stopper".

Analytical techniques, including assessment of initial spin test data, indicates the maximum local tensile stress in the blade is a highly localized surface stress of 43 KSI in the attachment area which reduces rapidly to a value of about 14 KSI at the centerline slightly below the minimum root width.

Flexure strength is measured with ceramic materials with a 3-point or a 4-point Flexure-Strength Test Fixture (the latter is shown as Figure 10). Initial flexure strength tests of Hot-Pressed Si_3N_4 indicate that the localized surface stress of 43 KSI which would occur at an attachment temperature of 1300°F is well within the capability of the material. The tensile data indicating the stresses across the root width could also be accommodated is shown in Figure 11. Additional materials characterization tests are being conducted to provide sufficient data for accurate statistical analyses.

The life-limiting component based on analysis of early test data is the HPSN first-stage blade, which is limited by creep rupture to 210 hours with a 2200°F gas path temperature. Creep-rupture life of the second stage blade is 600 hours. This creep life limitation is attributed to the previously discussed high temperature fluidity of the silicate phase of MgO at the grain boundaries. Clearly work with improved densifying additions for hot-pressed Si_3N_4 is strongly justified. While creep rupture will not be a problem for the 60 hour demonstration, there is additional concern for the effects of oxidation and hot-corrosion on materials properties as a function of exposure time.

CERAMIC COMBUSTION CHAMBER DESIGN

Design of a ceramic annular combustor maintaining the T76 engine combustor envelope and fuel system involved 3 basic design concepts. Initial designs used a metal dome and ceramic inner and outer concentric cylinders with ceramic transition pieces to complete the structure and direct the combustion gases to the turbine. Designs of the ceramic cylinders investigated include monolithic, barrel stave and stacked rings. The first step was to determine the thermal gradients in the cylinders.

The uncooled metal combustor coated with thermal paints, which was tested to establish typical combustor wall temperatures and thermal gradients, is shown in Figure 12. This testing indicated that a ceramic combustor would have a maximum wall temperature of 1700°F and a maximum thermal gradient of 800°F/inch.

Materials were analytically evaluated to survive the design conditions. The initial candidate material, siliconized SiC, had a low probability of success. RBSN and HPSN appear to be viable materials.

Preliminary designs of monolithic cylinders employing 3-D finite element stress analysis with typical combustor hot-spot patterns were analyzed. As one would expect, the inside surface of the cylindrical combustor expands axially but is constrained by the cooler outer surface. The thermal gradient through the combustor wall thickness places the hotter interior surface in compression and the cooler exterior section in tension. A peak stress of 28.5 KSI was determined at the longitudinal sides of the outer surface. This maximum tensile stress exceeded the strength capability of the siliconized SiC.

A more precise monolithic combustor outer wall model with cooling air holes was constructed using 3-D finite element analysis as shown in Figure 13. The particular model illustrated is a one-tenth circumference segment with three rows of 0.175 inch diameter cooling holes, 40 holes to the row. The wall thickness was 0.22 inches. The same thermal pattern was improved and was used in the preliminary analysis. A peak stress of 54.6 KSI was determined in a similar location as the configuration without holes. Thus, in this particular monolithic combustor wall, the peak axial stress was essentially doubled by the introduction of cooling holes.

These 3-D stress analyses were run for RBSN and HPSN. The maximum axial stress without holes for the RBSN and the HPSN were 9.5 KSI and 6.5 KSI respectively. The probability of success was 99.9% for the RBSN

and 92.1% for the HPSN. The lower thermal stress values for the RBSN results from its having the lowest values of modulus of elasticity and thermal expansion coefficients. If the stress concentration factor of 1.92 determined with the siliconized SiC was applied to the designs with HPSN and RBSN, then the peak stresses exceed the materials strengths of these materials. Thus, the probability of successfully operating an annular combustor with cooling holes constructed of concentric one-piece cylinders with siliconized SiC, RBSN or HPSN did not appear promising (6).

Preliminary analysis of an axial slat or barrel stave configuration was conducted using the same thermal pattern. A configuration of 20 staves, 0.22 inch thick with a length of the combustor was investigated. A peak axial stress of 34.3 KSI was obtained with siliconized SiC. This higher stress determined with the one-piece cylindrical wall was attributed to there being a smaller amount of material on the sides of the staves to react to the thermal strain created by the higher temperature on the wall inner surface. These stress levels suggested efforts be concentrated on the stacked ring configuration. British success at Lucas Aerospace with a stacked ring annular combustor also suggested more extensive assessment of this technique.

Two stacked ring designs are shown in cross section in Figure 14. One design uses axial springs to hold the assembly together in compression. The initial stacked-ring configuration analyzed consisted of four stacked rings. Again a one-tenth segment of the combustor outer wall circumference was used in a 3-D finite element analysis. The tangential stress peak with siliconized SiC was 18.0 KSI at the aft side of the inner surface of the second ring. The axial stress was 4.2 KSI. A similar analysis with RBSN determined the maximum axial stress was 1.5 KSI and 6.6 KSI for the maximum tangential stress. HPSN was run on the same model wherein the maximum axial stress was 4.9 KSI and maximum tangential stress was 35.1 KSI. The probability of success with both RBSN and HPSN was $\geq 99\%$ while the siliconized SiC was about 6%.

The stacked ring annular combustion chamber design was refined with variations in wall thickness, ring width, and cooling hole patterns. Stress levels were reduced by more than half when the ring width was reduced from 1.5 to 0.75 inches. Hot-spot location was more sensitive with the smaller ring width. Variations in the temperature distribution within the stacked ring did not significantly affect the probability of success. Addition of half-holes to the stacked ring configuration resulted in stress concentrations of 1.3 to 1.6. The analytical models used, showing the cooling hole patterns, are illustrated in Figure 15.

At this point in time, analysis has shown that a viable annular combustor can be made with RBSN or HPSN using the stacked ring concept with half circle cooling holes. A series of combustor rings has been ordered for evaluation testing in a combustor test rig.

CERAMIC COATINGS

Many of the advantages of ceramic materials in gas turbine hot-section applications can be obtained using ceramic coatings. Thus, the metal members would carry the structural load and the ceramic coating would provide corrosion/oxidation protection and thermal insulation. The problem is to accommodate the stresses generated by the inherent thermal expansivity mismatch during engine thermal excursion. Zirconia is a good candidate for a ceramic coating as it has one of the closest thermal expansivity matches of a ceramic to a metal superalloy.

There are three basic techniques of distributing the thermal mismatch stresses of the ceramic coating on a metal. A metal interlayer can be graded with a ceramic. The metal component would be gradually reduced and the ceramic component increased until a pure ceramic outer-layer is achieved. A second approach is to use a ductile interlayer to accommodate the mismatch stress. Another method would be to deposit the ceramic in a columnar type structure that could withstand the mismatch stresses. These techniques or a combination of them have been the primary techniques investigated.

Considerable progress has been made with plasma sprayed ceramic coatings. The annular combustion chamber on the FT 9 has a graded cobalt chromium aluminum yttrium (CoCrAlY), magnesia (MgO) stabilized zirconia (ZrO_2) as a bill of material thermal barrier coating as shown in Figure 16. This type of coating is bill of material on several production engines. The problem of coating a turbine airfoil is more difficult due to the geometrical problems associated with the airfoil contours. There has been some significant progress with plasma sprayed coating of NiCoCrAlY and ZrO_2 with discrete interface. The structure of the somewhat porous ZrO_2 structure appears to aid in the thermal stress accommodation. A nominal 15 mil. coating of this has successfully undergone over 500 engine cycles up to full power on a complete set of first stage blades in a J-75 gas turbine engine at NASA-Lewis (7).

NAVSEA has supported combined mode DC-RF sputtering at Battelle-Northwest to develop graded metallic-ceramic coatings for turbine airfoils. These coatings have been concentrating on achieving tight packed ceramic coatings which prevent diffusion of corrosive agents through the coating. This work is quite promising. NAVSEA is initiating a program to develop a ceramic coating for naval applications wherein plasma spray and sputtered coatings will be comparatively evaluated. Preliminary plasma spray coatings are shown on airfoils ready for engine test stand evaluation in Figure 15. The NAVSEA program

involves considerable materials development to optimize the coating and engineer the coating for specific airfoils. At-sea engine testing will be used to evaluate the developed ceramic coatings.

SUMMARY

Ceramic materials hold tremendous potential improvement for use in marine gas turbine engines. The aspects of ceramics the Navy is particularly interested in include improved hot-corrosion resistance, elimination of turbine blade showerhead cooling requirements, improved engine power output and efficiency, greater tolerance for a wider range of fuel types and contamination levels, and reduction in the use of critical materials.

Although ceramic materials are brittle, the non-fragile, high-strength ceramics based on silicon, nitrogen and carbon are of particular interest for engine use. The problem with ceramics is that the materials do not undergo plastic deformation before fracture as is the case with metals. Thus, components have to be designed with low magnitude localized stress concentrations.

DARPA tasked NAVSEA/NAVSEC to technically manage a ceramic demonstrator engine program with Garrett. This program entails modifying the T76 gas turbine engine such that the first and second stage turbine stator and rotor airfoils, the shrouds and the combustion chamber are made of ceramic materials. The program is structured to have an engine in 3 years operating with turbine inlet temperatures up to 2200°F. A success criteria was defined as 50 hours cyclic test stand operation followed by 10 hours in a boat. This time constraint dictates use of materials which have been fairly well characterized and adaption of design approaches which have shown promise on earlier programs. Thus, the Garrett program will involve integration and extension of the 1976 state-of-the-art ceramic technology. Hot-pressed silicon nitride is the primary candidate for first and second stage blades and reaction bonded silicon nitride was chosen for the vanes, shrouds, transition liners and combustion chamber.

The major work at this point has been in design. A much higher level of precision in analysis is required in design to minimize localized stress concentrations than is necessary with metal engine design. Stress modeling using 2-D and 3-D finite element stress and thermal analysis were used with the ceramic components. This analysis, coupled with probabilistic statistical treatment of ceramic materials data and successive iterations, was used to develop analytical designs which have a high theoretical probability of success. Extensive component development testing is being used in conjunction with the analytical techniques to fine tune the design. Cold and hot spin tests have been conducted to verify the ceramic blade attachment to metal disk. The initial test results have been very promising.

Combustor analysis has indicated a stacked ring approach forming the inner and outer cylinders of the annular combustor should meet the program objectives. Siliconized SiC would not be satisfactory. Both RBSN and HPSN theoretically would be adequate. Fabrication capability favors the RBSN. Testing in the combustor rig will be used to finalize the design.

The durability of the ceramicized T76 engine limits its consideration for naval applications. This engine should be considered as an evolutionary step in the revolutionary use of ceramics as structural members of the hot-section. This program will provide needed guidance for advanced development of ceramics. Navy use of ceramics as short life propulsion engines in RPV's and missiles, ceramic bearings and diesel engine pistons may well see Fleet introduction in the 1980's. Production ceramic gas turbines competitive with metal engines are probably on the order of 20 years away.

REFERENCES

- (1) Committee on the Use of Ceramics in Industrial Gas Turbines, "Concept Feasibility Study of Ceramics for Use in Electric Utility Gas Turbine Fired with Coal Derived Fuels", ERDA Final Report SETEC DO 76-024F October 1976, University of Pittsburgh
- (2) Godfrey, D. J. "The Properties of Silicon Nitride Ceramics and Their Use in Service Thermal Environments", Admiralty Materials Laboratory Report No. 1/75, Holton Heath, England, February 1975
- (3) Gazza, G. E., "Hot-Pressed Si_3N_4 ", Journal of American Ceramic Society, 56, 662 (1973)
- (4) McLean, A. F., Bratton, R. J., "Brittle Materials Design, High Temperature Gas Turbine", Interim Report No. 10, Contract DAAG 46-71-C-0162 with DARPA, Dearborn, MI, October 1976
- (5) Wallace, F. B., Nelson, N. R., "DARPA/NAVSEA Ceramic Gas Turbine Engine Demonstration Program", Report No. 3, Garrett AiResearch, Phoenix, AZ, December 1976
- (6) Wallace, F. B., Nelson, N. R., "DARPA/Navy Ceramic Engine Progress", ERDA Workshop, Orlando, FL, January 1977
- (7) Levine, R. S., Clark, J. S., "Thermal Barrier Coatings, A Near Term High Payoff Technology", Proceedings on Workshop on Ceramics for Advanced Heat Engines, ERDA, Orlando, FL, January 1977
- (8) Rice, R. W., McDonough, W. J., "Hot-Pressed Si_3N_4 with Zirconia Base Additives", Journal of American Ceramic Society, 58, 264, May-June 1975

LIST OF FIGURES

FIGURE	TITLE
1	Relative Temperature Capabilities of Advanced Metal Alloys and Ceramics
2	T76 Gas Turbine Engines
3	Ceramic Hot-Section Component Modification to T76
4	DARPA/NAVSEA Ceramic Demonstrator Gas Turbine Engine Program Schedule
5	Technical Review Panel - Ceramic Gas Turbine Demonstrator Engine Program
6	Thermal Model - First Stage Blade and Metal Disk Attachment Region
7	2-D and 3-D First Stage Blade Analytical Models
8	Second Stage Blade Principal Stress at 41,730 RPM (Maximum Stress in KSI)
9	Spin Pit Disk and Attachment Configuration
10	4-Point Flexure Strength Test Device
11	Tensile and Flexure Strength Data of Silicon Nitride
12	Metal Combustor with Thermal Paint Isotherms Used to Determine Hot-Spot Patterns
13	Outer Combustor Wall, 3-D Finite Element Model
14	Stacked Ring Combustor Assembly
15	Stacked Ring Analytical Model
16	Plasma Sprayed Graded Metallic-Ceramic Coating on FT9 Combustion Chamber
17	Plasma Spray Coatings on Blades for Engine Test

TABLE I: Some Physical Properties of Silicon Nitride

<u>Property</u>	<u>Value</u>	<u>Comments</u>
Melting Point	Vaporizes at about 1900°C	
Density	2.2 to 3.2 g/cm ³	depending on method of fabrication
Coefficient of Thermal Expansion to 1000°C	2.46 to 4.1 x 10 ⁻⁶ °C ⁻¹	variation in investigators
Young's Modulus	up to 46 x 10 ⁶ psi 29 x 10 ⁴ MN m ⁻²	depends on fabrication
Modulus of Rupture	up to 125,000 psi 860 MN m ⁻²	depends on fabrication
Thermal Conductivity	up to 20 Btu hr ⁻¹ ft ⁻¹ °F ⁻¹ 36 watts m ⁻¹ °K ⁻¹	depends on fabrication
Specific Heat	0.17 cal/g°C 0.712 kJ/kg°C	
Hardness	1600-1800 Vickers VPN >9 (Moh)	
Electrical Resistivity	greater than 10 ¹⁰ ohm cm	

(Croft and Cutler, "Review of Silicon Nitride", ONR Report No. R-16-73, July 1973)

TABLE II: Some Physical Properties of Silicon Nitride

Method of Fabrication	Porosity (in percent)	Coefficient of Thermal Expansion (cm/cm/°C)	Young's Modulus (in psi)	Modulus of Rupture (in psi)
Reaction Sintered	31%	2.5×10^{-6}	8×10^6	28,000
Reaction Sintered	18%			
Hot Pressed	~0		41.5×10^6	82,000
Reaction Sintered	25%	3.2×10^{-6}	25×10^6	42,000
Hot Pressed	~0	3.2×10^{-6}	46×10^6	125,000

(Croft and Cutler, "Review of Silicon Nitride", ONR Report No. R-16-73, July 1973)

TURBINE AIRFOIL LIFE IN MARINE GAS TURBINES

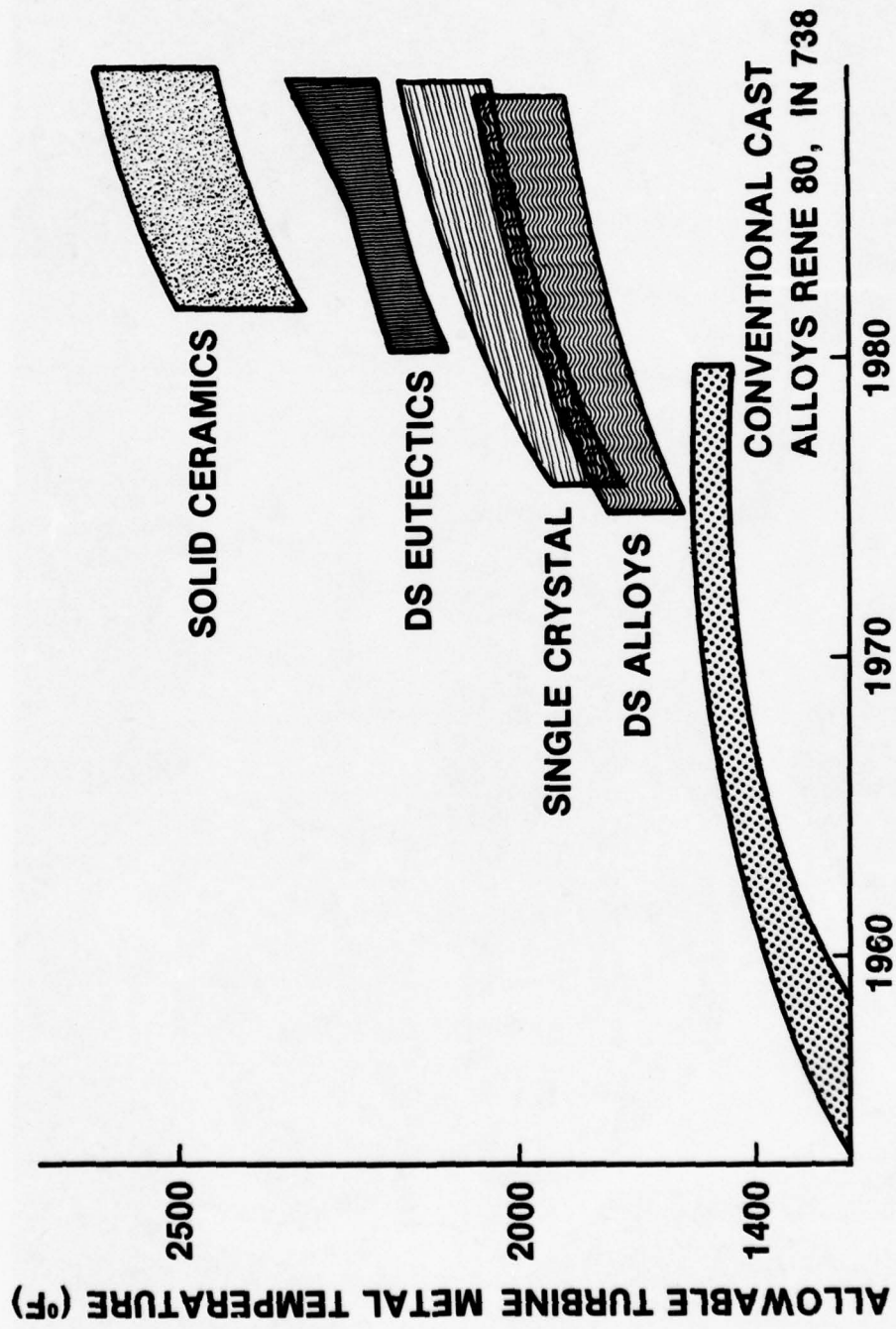


FIG. 1

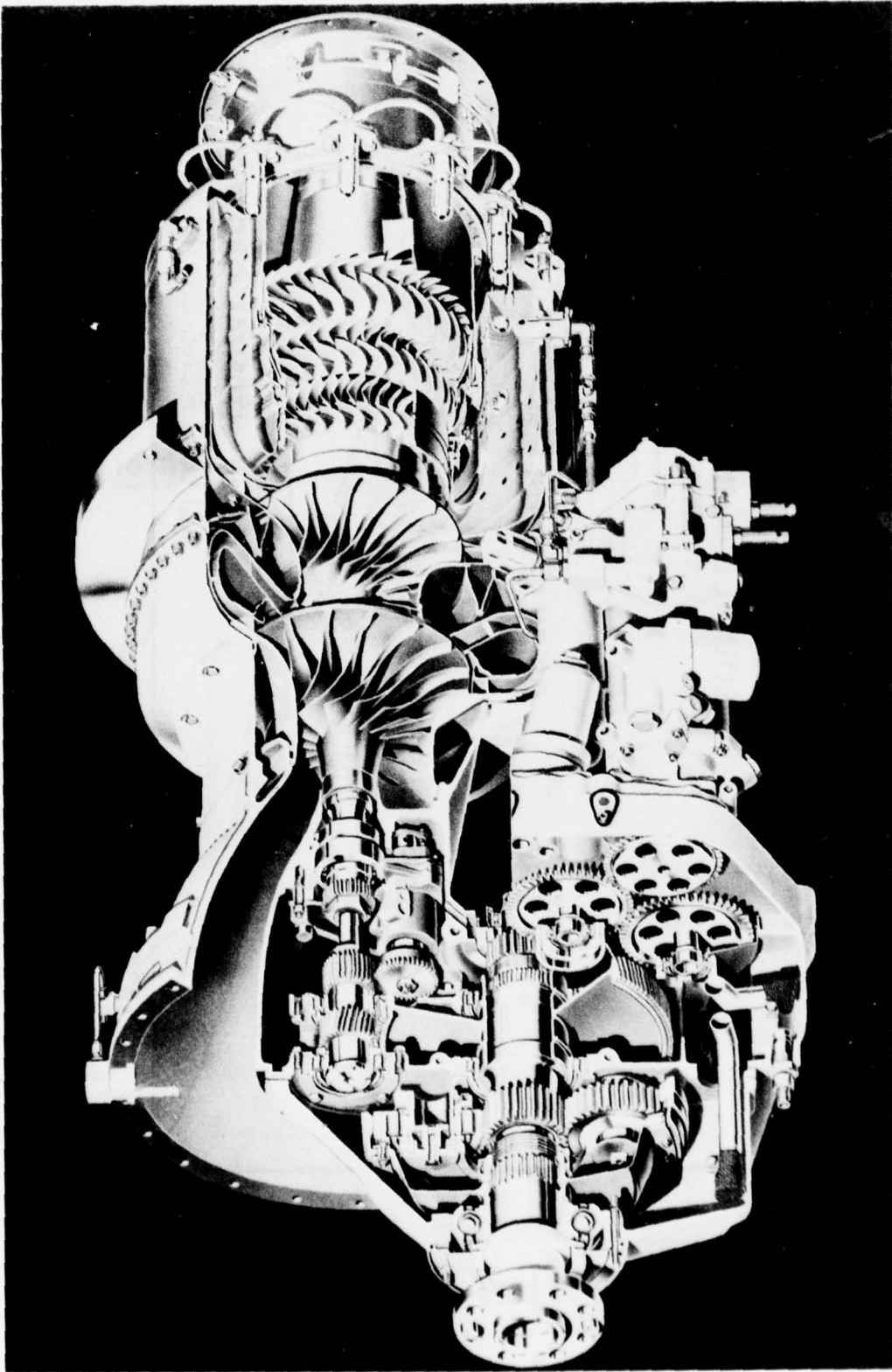
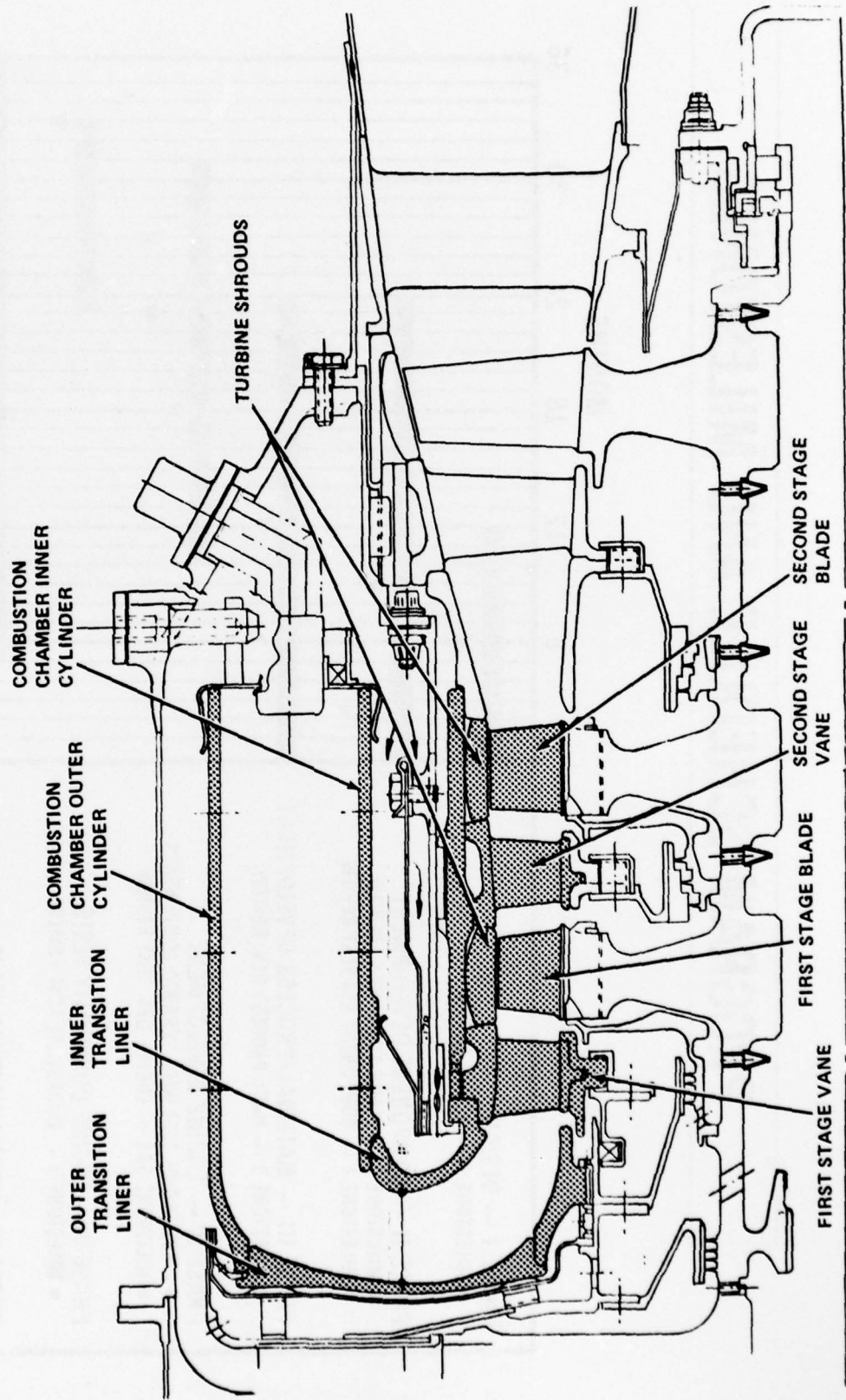


FIG. 2

FIGURE 3 CERAMIC HOT-SECTION COMPONENTS



PROGRAM SCHEDULE AND MILESTONES

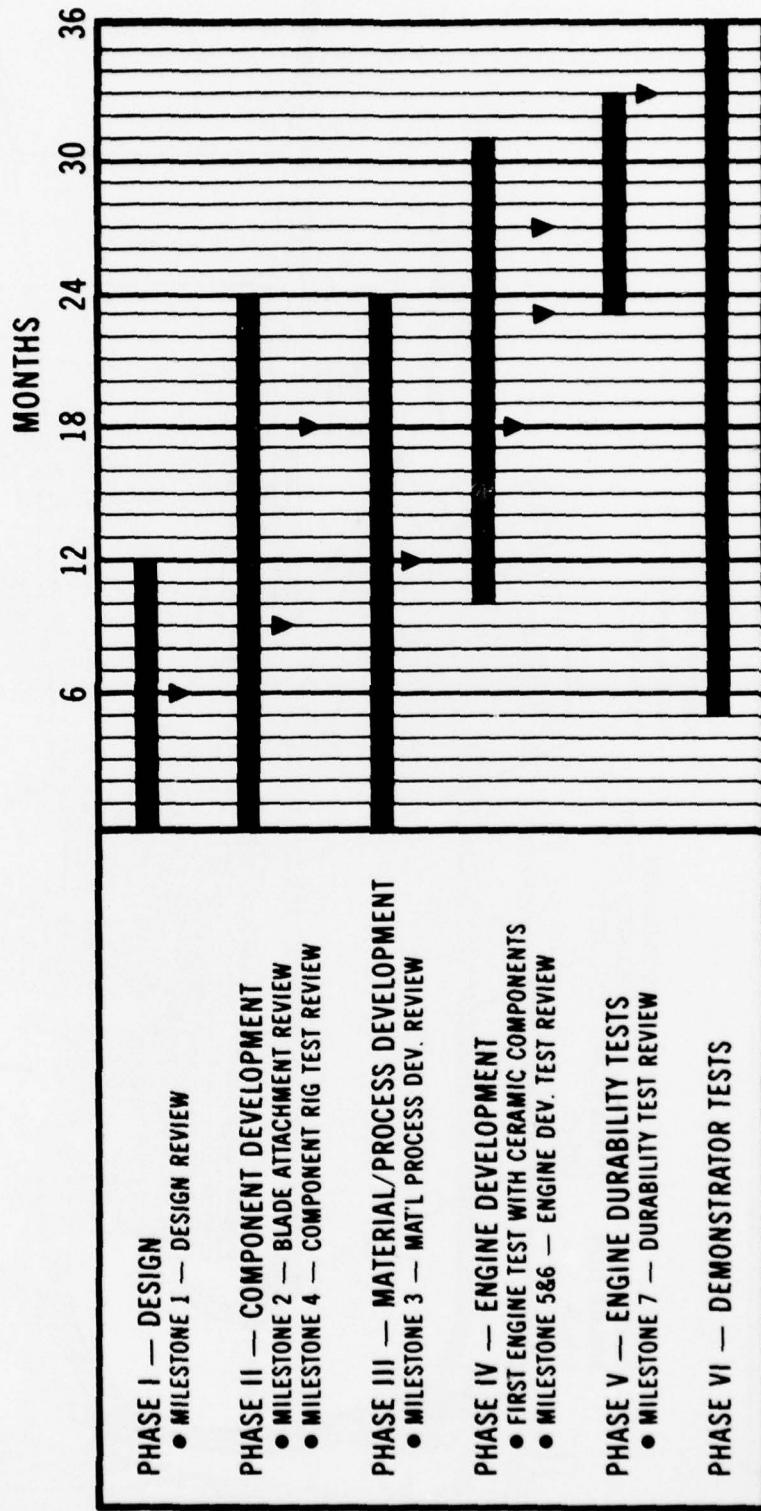


FIG. 4

CERAMIC DEMONSTRATOR GAS TURBINE ENGINE PROGRAM TECHNICAL REVIEW PANEL

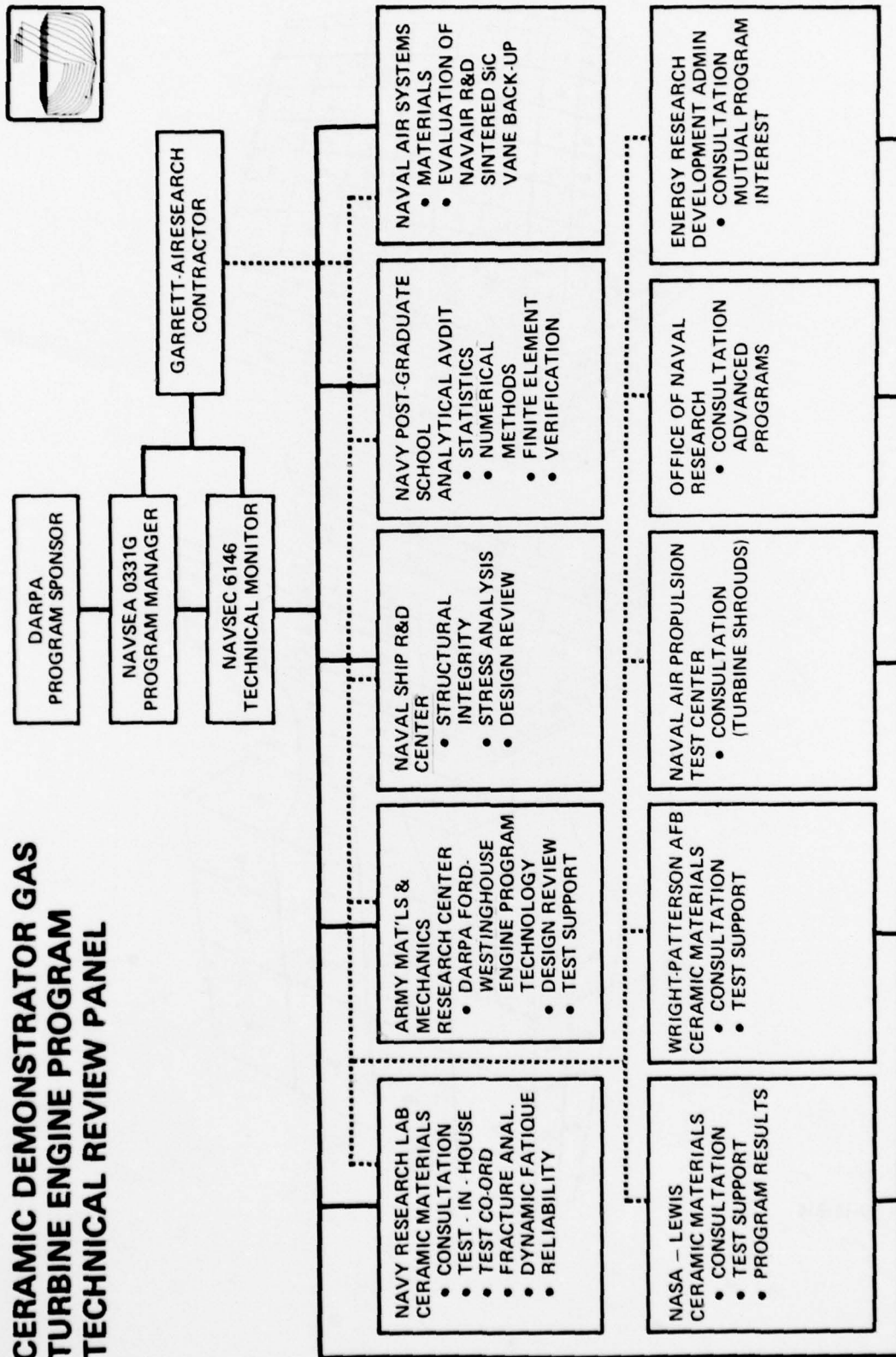
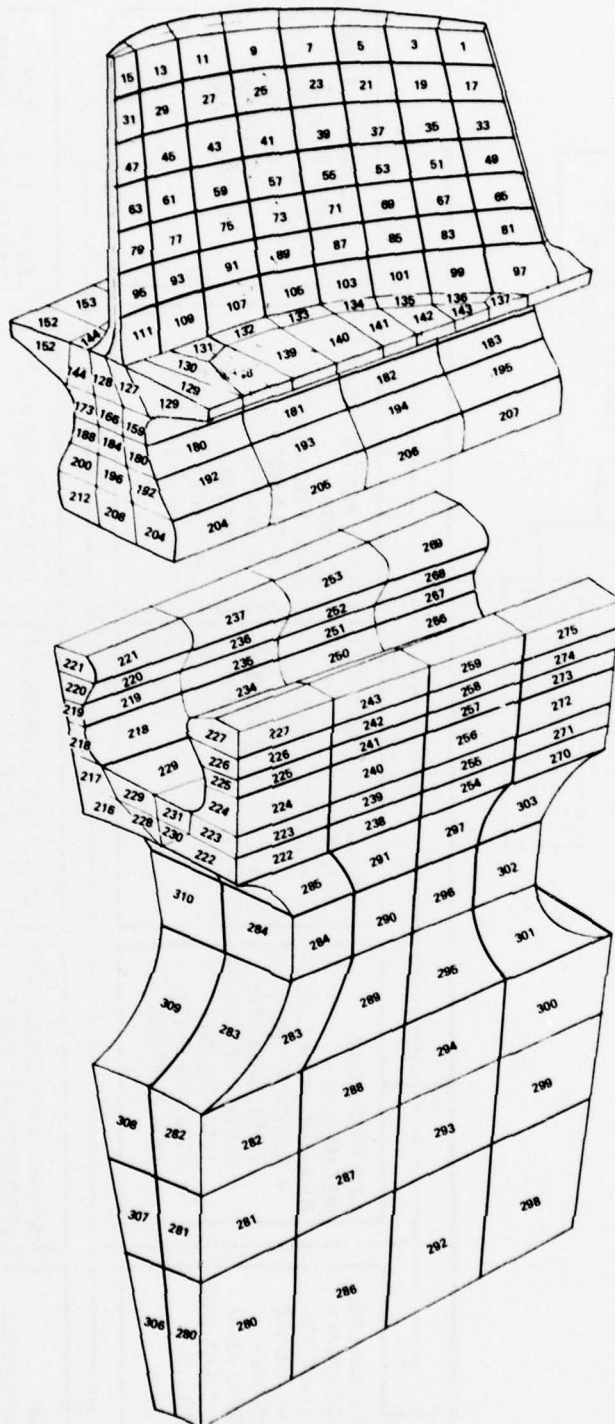
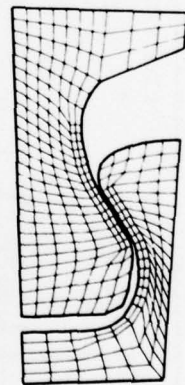
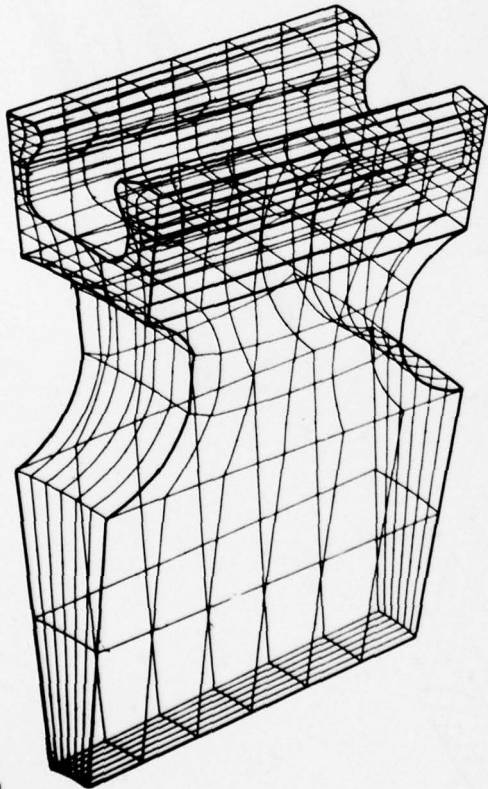
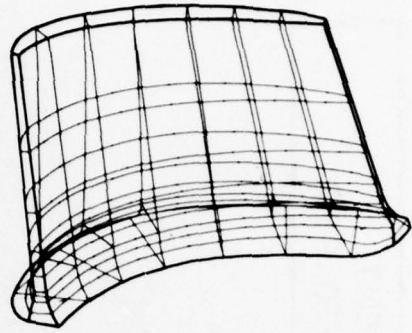
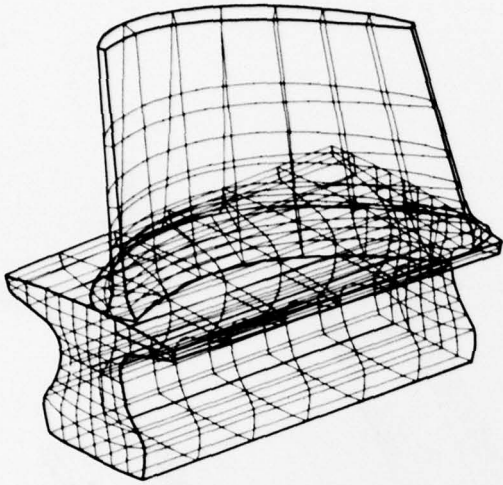


FIG. 5



M6-15-234

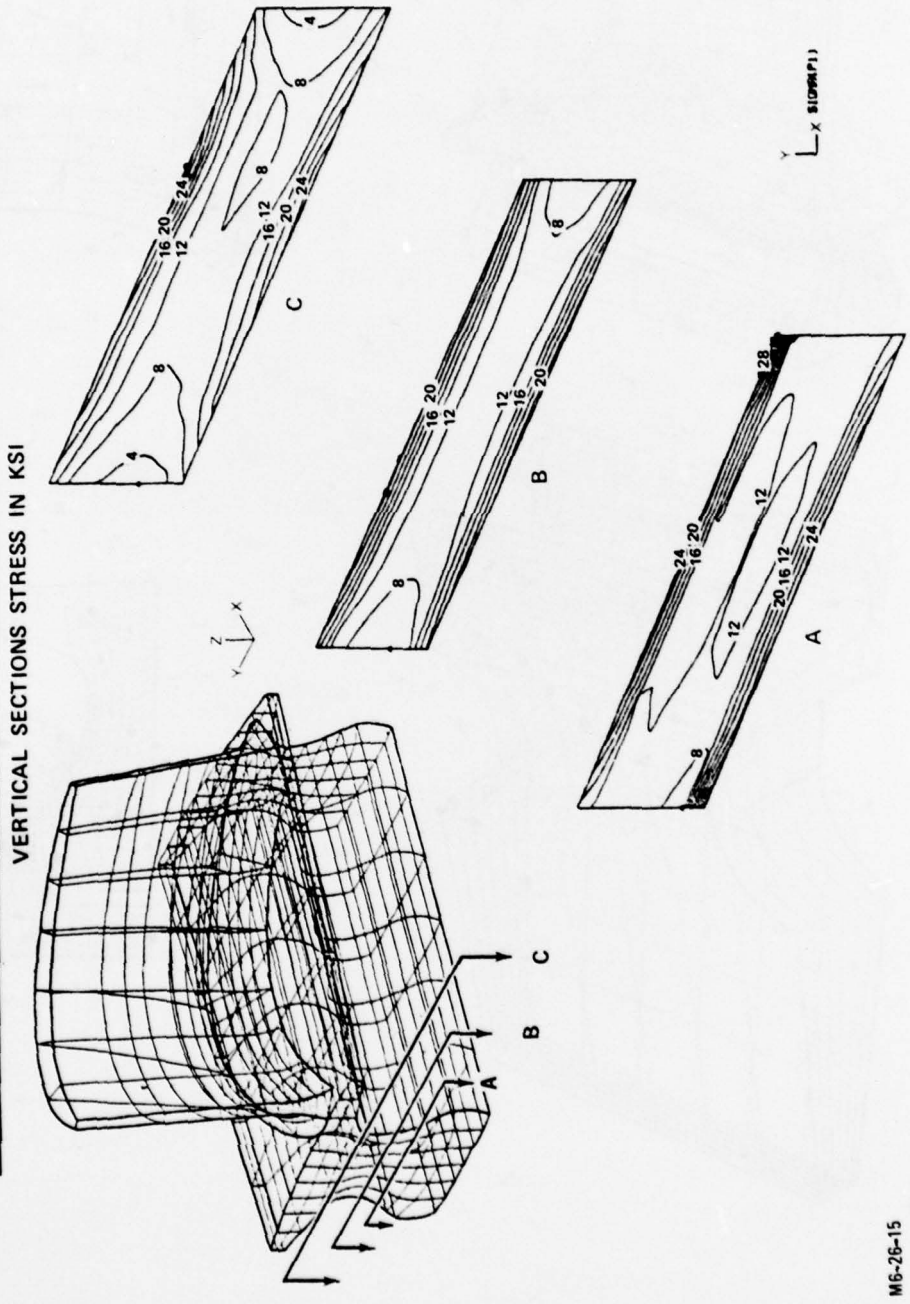
FIG. 6



MG-15-51

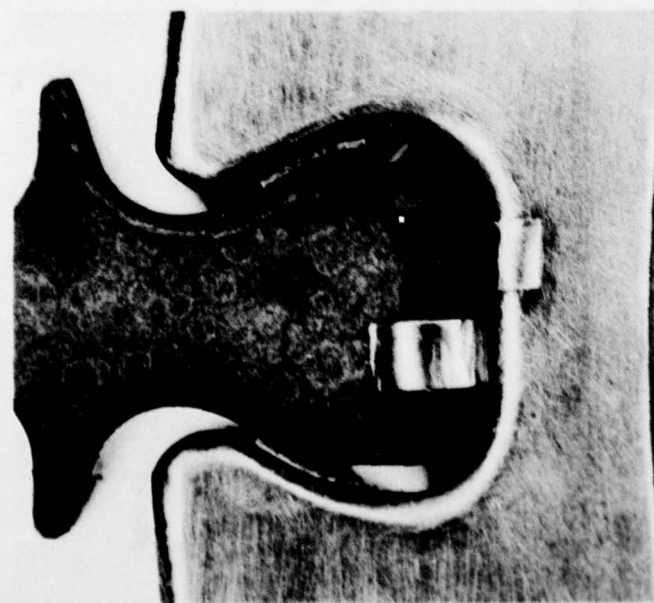
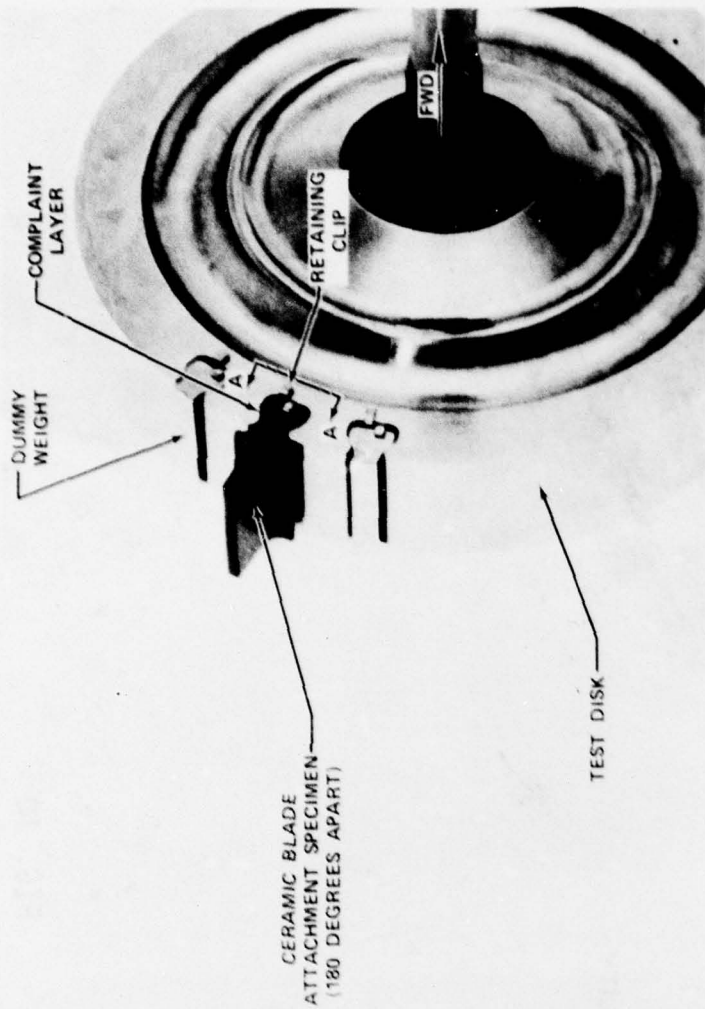
FIG. 7

**SECOND-STAGE BLADE ATTACHMENT
MAXIMUM PRINCIPAL STRESS AT 41,730 RPM**



MG-26-15

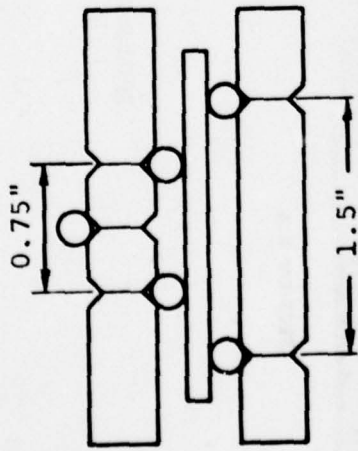
FIG. 8



SECTION A-A

SPIN-PIT DISK AND ATTACHMENT CONFIGURATION

FIG. 9



SCHEMATIC SHOWING SELF-ALIGNING CAPABILITY

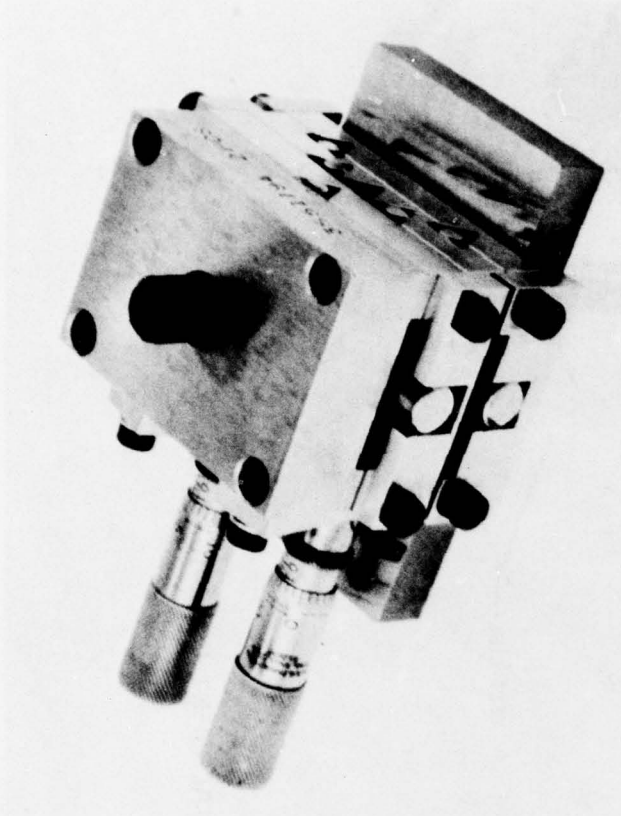


FIG. 10

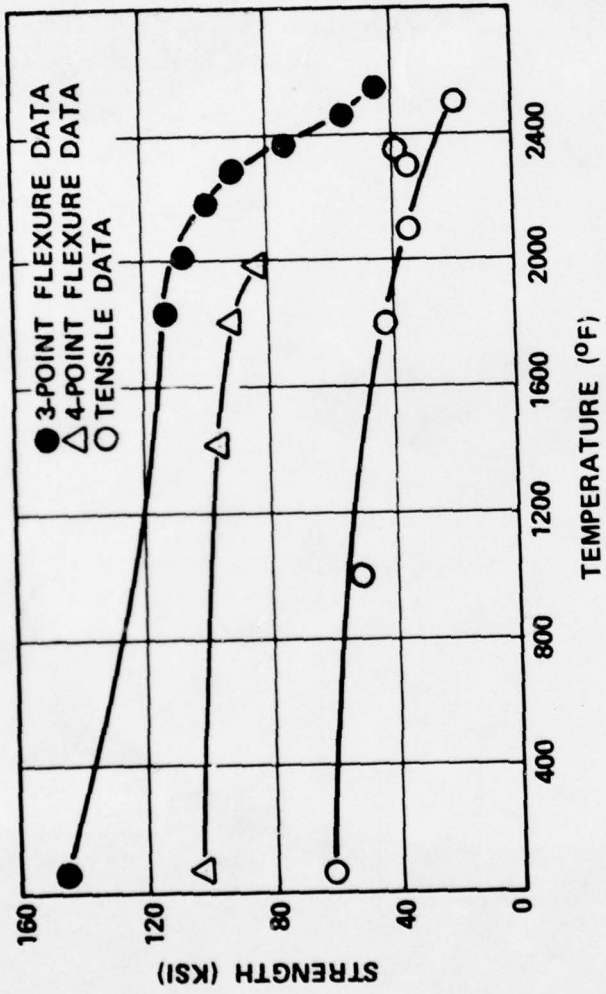


FIG. 11

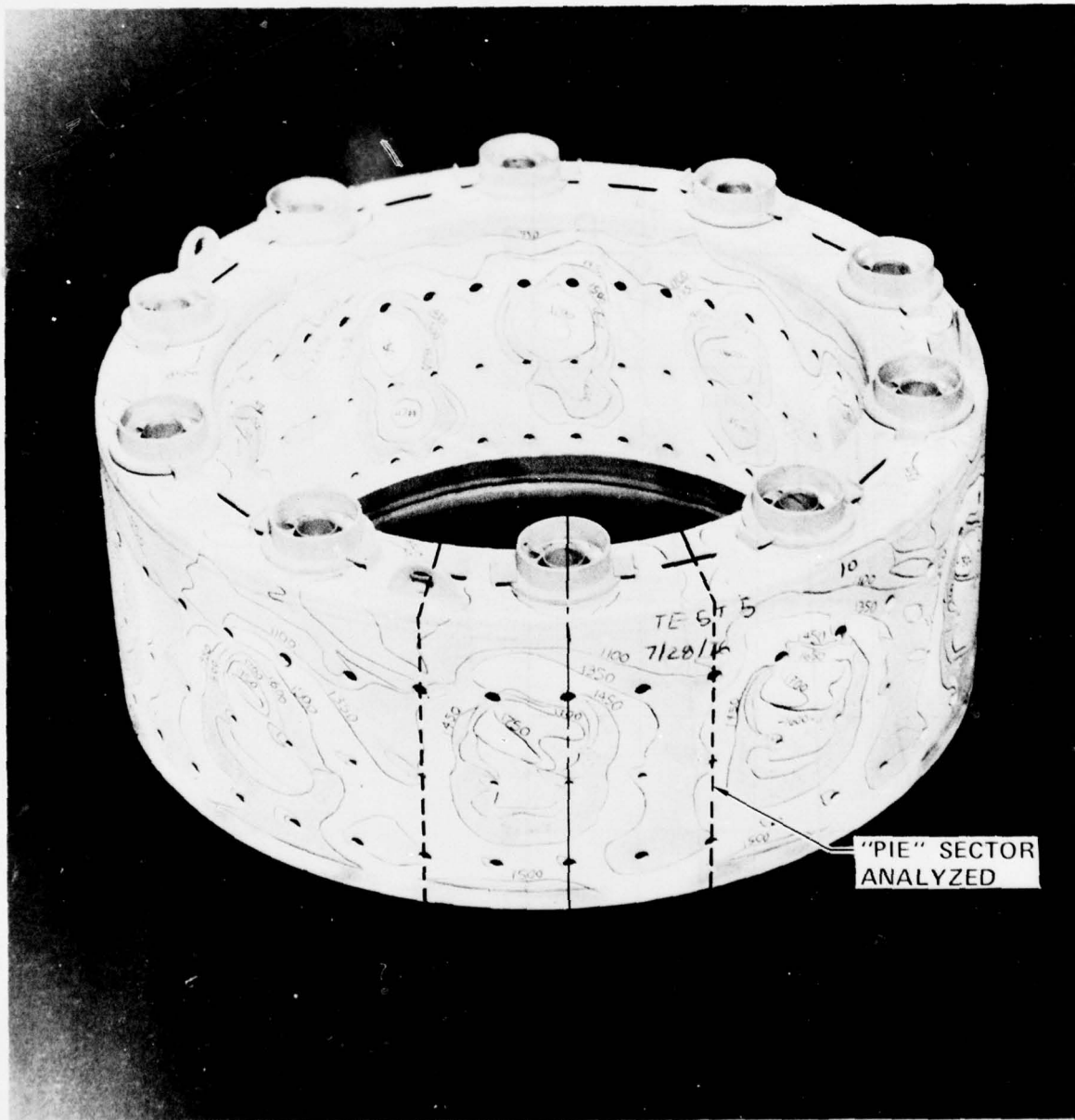


FIG. 12

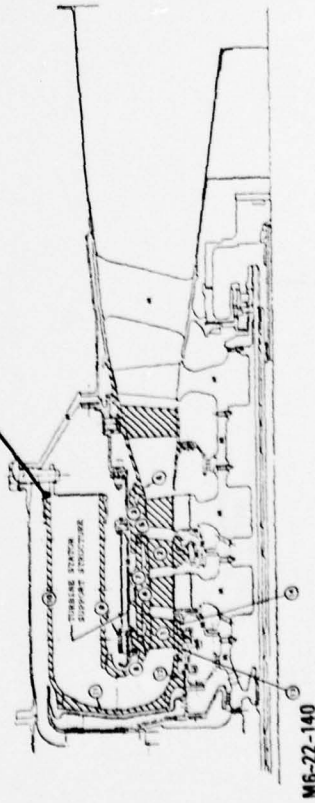
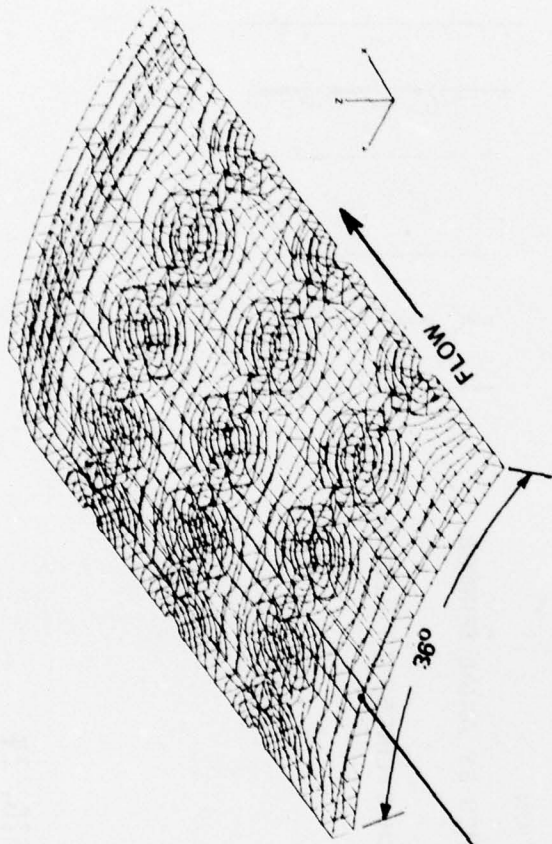
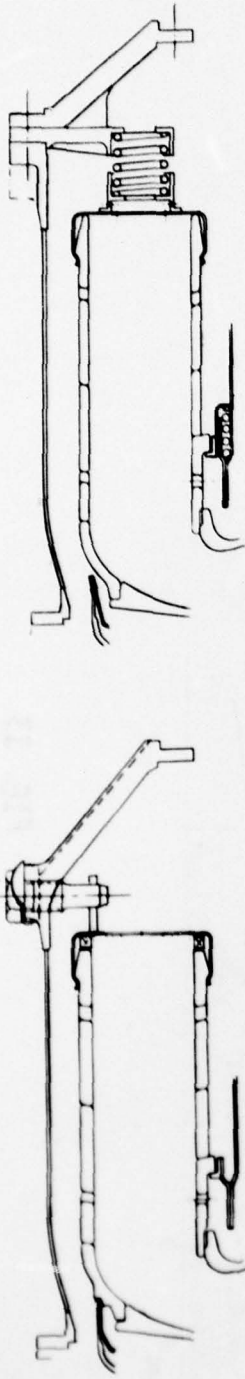
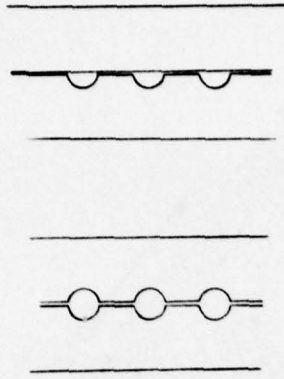


FIG. 13

M6-22-140



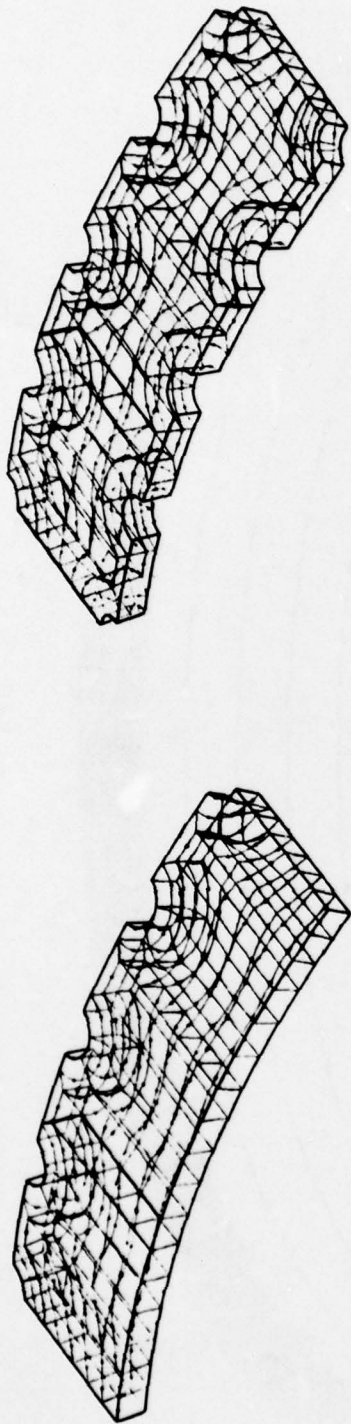
- STACKED RING CONFIGURATION.
- ASSEMBLY CLAMPED TOGETHER BY AXIAL SPRINGS.
- ORIFICES ON EDGES OF EACH CYLINDER TO REDUCE STRESSES.



M6-22-166

FIG. 14

3-D FINITE ELEMENT STRESS MODEL - STACKED RINGS WITH HOLES



M6-22-152

FIG. 15

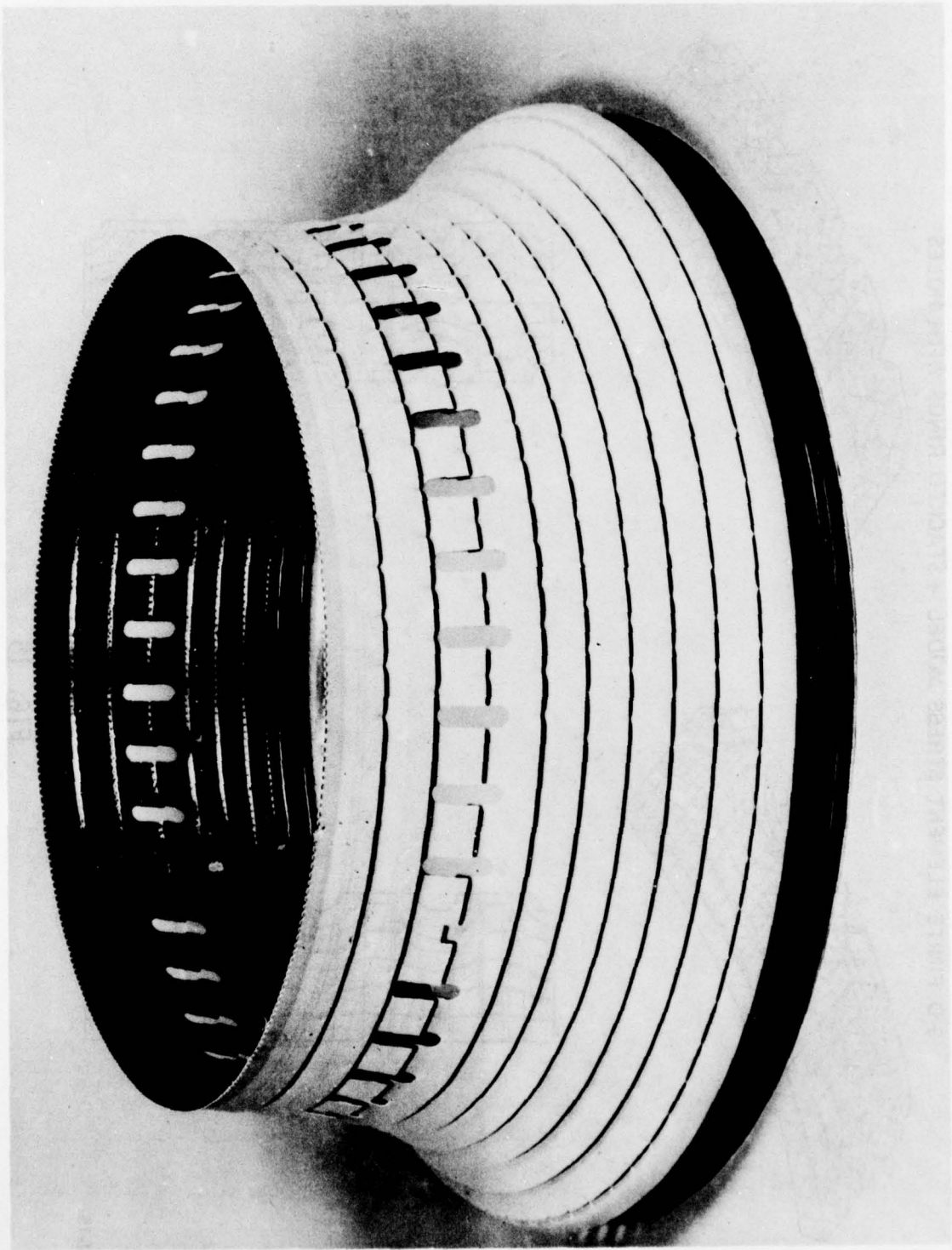


FIG. 16

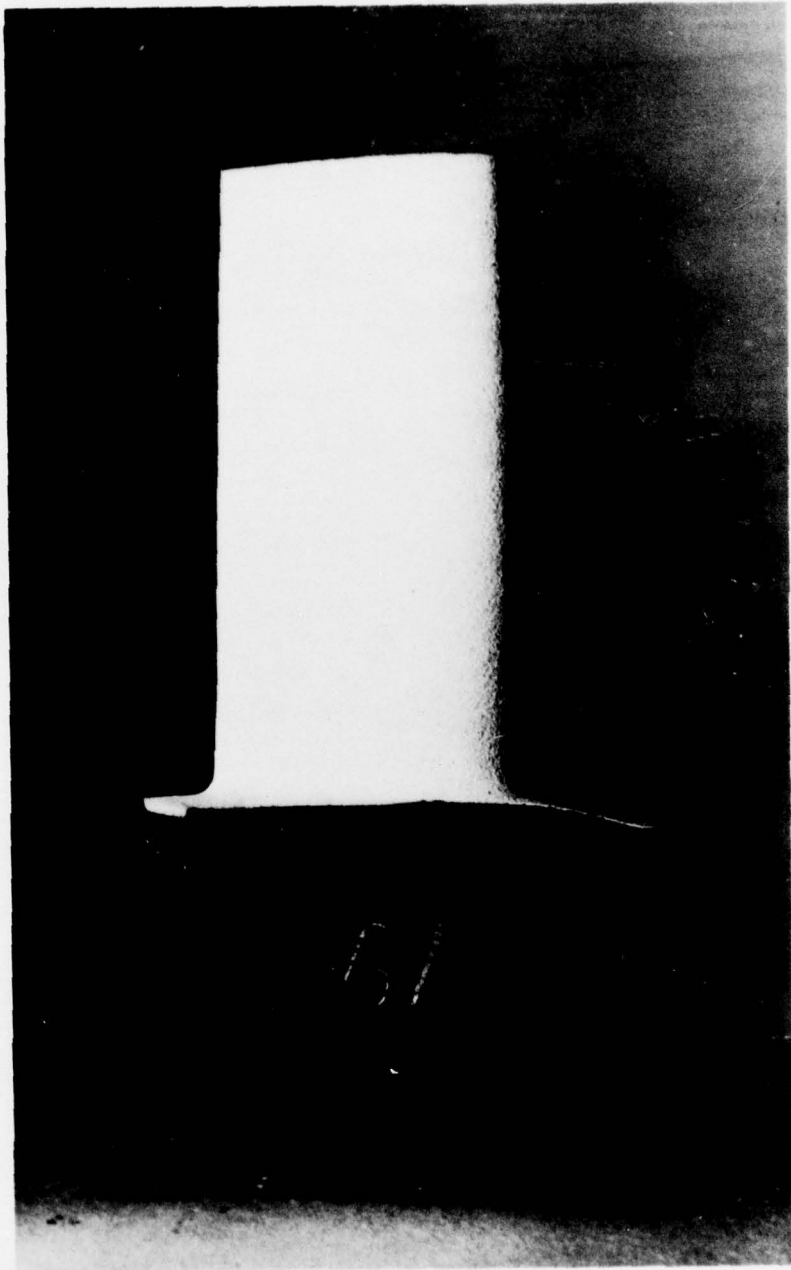


FIG. 17